Restoring forces in cardiac myocytes

Insight from relaxations induced by photolysis of caged ATP

E. Niggli and W. J. Lederer

Department of Physiology, University of Maryland School of Medicine, and the Medical Biotechnology Center, Baltimore, Maryland 21201 USA

ABSTRACT Concentration jumps of intracellular ATP were produced by photolysis of P^3-1-(2-nitrophenyl)ethyl (NPE)-caged ATP and were used to investigate the passive relengthening properties in unloaded cardiac myocytes. Patch–clamp pipettes in the whole-cell mode were used to voltage-clamp the myocytes and to load the cells with caged ATP while optical methods were applied to record sarcomere length or cell length simultaneously. Cell length was varied using energy deprivation contractures while intracellular Ca^{2+} was controlled with EGTA. At sarcomere lengths between 1.8 and 1.4 μm cellular relengthening after photolysis of caged ATP was rapid ($t_{1/2} \approx 100$ ms) and could be well described by a simple mechanical model. However, ATP jumps made at sarcomere lengths ~1.1 μm led to slow relengthening ($t_{1/2} \approx$ seconds), comparable to the slow reextensions observed in skinned myocytes after bulk solution changes. We attribute the slow and incomplete relengthening of intact and skinned myocytes after severe rigor shortening to deformation and alteration of structural elements inside the cell. Relengthening from intermediate sarcomere lengths in intact cells is elastic and provides information about the underlying relengthening forces inside the cell. The data do not support the presence of a significant discontinuity in elastic modulus at a sarcomere length of ~1.6 μm expected from ultrastructural features of the sarcomeres and from observations in skinned myocytes. Our results suggest that the cell length measurements usually performed in this preparation provide an adequate description of the force produced by the unloaded cell in the steady state. The results also provide a way to estimate the error arising from viscous forces during rapid shortening.

INTRODUCTION

The unloaded isolated cardiac myocyte has been successfully used as a preparation for physiological and biophysical experiments exploring a wide range of cellular functions. For example, it is well suited for the characterization of membrane currents using the giga-seal technique in the whole-cell recording mode (1). The regulation of subcellular ionic concentrations can be investigated using ion-specific fluorescent indicators in conjunction with fluorescence-microscopy (2, 3). Mechanical properties and the contractile behavior of isolated cardiac myocytes can be studied as well in field-stimulated or voltage-clamped cells. Several parameters, including cell and sarcomere length, have been measured to obtain information about the mechanical properties of heart cells (4, 5). However, force measurements under isometric conditions have not routinely been performed in intact single cells (but see reference 6). Unfortunately, unloaded shortening provides rather indirect information about the actual force developed by the myocyte. However, relengthening after twitch contractions indicates the presence of an internal restoring force against which the "unloaded" cell has to produce force in order to shorten. The corresponding force–length relationship is unknown because the internal restoring forces cannot be easily measured directly in intact cells. In addition, the structural elements underlying this internal load are not precisely known. Results from skinned cells and from protein extraction experiments indicate important roles for the contractile proteins as well as other filamentous cytoskeletal elements (7).

Sarcomere length/tension data obtained with multicellular muscle preparations (see for example references 8 and 9) and considerations of the subcellular organization of the contractile proteins in the sarcomeres (10) suggest a nonlinear relationship between sarcomere length and internal restoring force in the range of sarcomere lengths prevailing in unloaded myocytes, giving rise to steeply increasing internal forces at sarcomere lengths $< \approx 1.6$ μm. Below this length the myosin filaments are expected to touch the Z-discs of the sarcomeres. However, even in multicellular preparations and in skeletal muscle fibers the quantitative contribution of internal loads to the decrease in force at sarcomere lengths < 1.9 μm is unclear. Other mechanisms have been suggested to play a more important role for the decline in force in the range of the ascending part of the force/sarcomere length relationship (e.g., length-dependent Ca^{2+} sensitivity of the contractile proteins and length dependence of the Ca^{2+}-release process [11]).

Dr. Niggli's present address is Department of Physiology, University of Berne, Buehlplatz 5, CH-3012 Berne, Switzerland.

0006-3495/91/05/1123/13 $2.00

Relengthening of unloaded myocytes depends on internal forces. The process of relengthening from a twitch contraction exhibits a complex multiexponential time course. In addition to the viscoelastic properties of the subcellular structures, several processes restoring the low resting calcium may be involved in relengthening, including the Na^+-Ca^{2+} exchanger and the Ca^{2+} pumps of the sarcoplasmic reticulum (SR) and the sarcolemma. These processes with different kinetics could be rate-limiting in the relengthening of unloaded cells (12, 13). Thus, the analysis of cell relengthening from normal twich contractions may not provide direct information about the passive viscoelastic properties of the cell.

Because the internal forces opposing shortening cannot be measured directly but their magnitude seems to be of crucial importance to the understanding of "unloaded" shortening in single cells, we have made use of a new approach to study the passive relengthening properties of isolated myocytes. We have obtained information about the passive relengthening force by examining reextension in the absence of Ca^{2+} activation of myofilaments. Energy deprivation contractures in the absence of extracellular Ca^{2+} and at low and buffered intracellular Ca^{2+} were induced by metabolic inhibition. The reduction of $[ATP]_i$ resulted in sarcomere shortening without increasing the intracellular calcium concentration (14). At any given sarcomere length achieved during the slow energy deprivation contracture, the shortening force was opposed by an equivalent internal restoring force of opposite direction. The contraction eventually proceeded until the increasing formation of rigor bridges and reduced number of cycling cross-bridges prevented further shortening. At this point, the rigor stiffness prevented the internal restoring force from relengthening the cell and the Ca^{2+}-independent cross-bridge cycling from further shortening the cell. A step increase in $[ATP]_i$ (produced by rapid photorelease of ATP from caged-ATP) led to relengthening, which could be analyzed without interference from forces related to changes in intracellular calcium concentration. The analysis was performed by modeling the passive relengthening system with a mechanical model including the cell mass and an elastic element damped by a viscous element. Preliminary results have been presented to the Biophysical Society (15).

METHODS

System overview

The superfusion chamber for single cells (16), the input optics, and the voltage-clamp headstage were arranged around the inverted Nikon Diaphot microscope (Nikon, Inc., Instrument Div., Garden City, NY) positioned on a vibration isolating table (Kinetic Systems, Roslindale, MA) inside a Faraday cage. The electronic equipment used to control the experiment and analyze the data was mounted in two racks near the Faraday cage. The flash units were located under the table in a partially open Faraday cage.

Voltage clamp and data acquisition

During the experiments, the cells were held at a fixed resting potential between −50 and −90 mV by the voltage-clamp amplifier (DAGAN Corp., Minneapolis, MN). To check for an unchanged low access resistance of the pipette in the absence of extracellular Ca^{2+}, voltage-clamp depolarizations to different potentials were applied every 60 s to evoke Na^+ inward currents. A low access resistance is important to facilitate loading of the cell with the caged compound by dialysis through the pipette tip. Fluorescent molecules of similar molecular weight have been shown to distribute homogeneously throughout the cytosol when loaded alone (3, 17). Control experiments have also indicated that the usual uniform distribution of the fluorescent calcium-sensitive indicator Indo 1 was unaltered when it was coloaded with a caged compound (data not shown), providing indirect evidence, that the distribution of caged ATP is uniform. Unlike ATP, caged ATP is not consumed by the cell and therefore, no maintained gradients can develop (see below for experimental significance of potential small nonuniformities of photoreleased ATP).

The experiments were controlled by a 80386 CPU-based computer (Dell Computer Corp., Austin, TX) running PClamp V5 software (Axon Instruments, Inc., Burlingame, CA). Data were acquired partially during the experiment and stored on disk. In addition, up to eight data channels were continuously recorded on video tape with a PCM encoder (Neurodata, Inc., New York, NY).

Input optics

The input optics, which were built by us around the microscope, were designed to allow the simultaneous use of a sarcomere length (or cell length) measuring system while carrying out UV-epifluorescence illumination for photolysis (see Fig. 1). The use of an epifluorescence illumination for photolysis prevents significant photolysis of caged

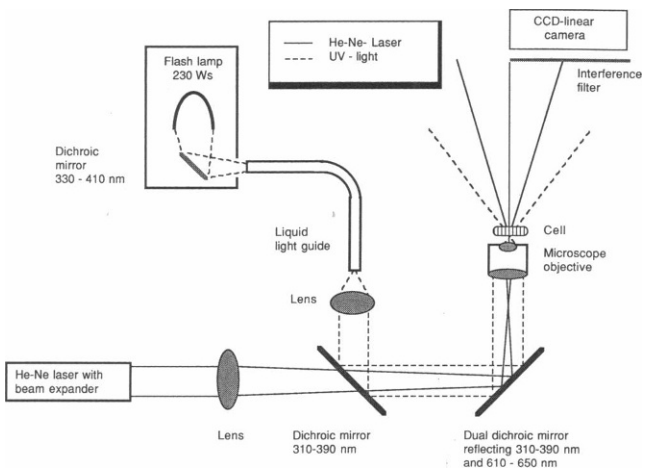

FIGURE 1 Optical pathway for flash-photolysis and laser diffraction. The same optical system was used for the sarcomere length measuring system (He–Ne laser light) and for the flash-illumination in an epi-illumination design (UV light). For a detailed description refer to Methods.

ATP in the patch pipette. Both the light flash for photolysis and the laser light for sarcomere length measurements used the same microscope objective (Neofluar Oel 63×, n.a. 1.25; Carl Zeiss, Inc., Thornwood, NY). The optical requirements of these applications were different, however. The system for sarcomere length measurments required a collimated narrow laser beam to leave the microscope objective. In contrast, the UV part of the input optics were configured to image the UV light source onto the preparation.

Sarcomere and cell length measurements

The mechanical activity of unloaded cells was measured with a laser diffraction system to determine the median of the sarcomere lengths or with a video dimension analyzer to assess cell length, which is a representation of the average sarcomere length as well. At the very short sarcomere lengths prevailing during extreme energy deprivation contractures, the laser diffraction system could not be employed because the diffraction pattern became faint. As judged from the dispersion of the first-order diffraction pattern, the usual subcellular distribution (18) of the sarcomere lengths was well maintained during energy deprivation contractures for sarcomere lengths between resting conditions and ~1.4 μm. Below this limit, the sarcomeres became undetectable with either method and significant nonuniformities of the sarcomere arrangement are likely to occur. However, in the range of sarcomere lengths prevailing during twitch contractions, both methods report the average sarcomere length within the cell with the resolution of the system. The laser diffraction system used has been described in detail elsewhere (19). Only the modifications necessary to make it compatible with the UV epi-illumination are outlined here. To optimize the required small beam diameter, the tradeoffs of the diffraction-induced beam divergence had to be taken into account. This divergence tends to increase the beam diameter at the position of the linear CCD camera (mounted 100 mm above the preparation to gain free access with the patch clamp electrode). Given the cell dimensions (100–150 μm × 15–20 μm) and the diffraction limits, a beam diameter of ~100 μm was calculated to be optimal. This diameter was achieved by expanding the beam diameter 10-fold before compression using a beam expander (Oriel, Stratford, CT). The expanded beam measuring ~10 mm in diameter was then focused with a planoconvex lens into the back focal plane of the microscope objective after passing a dichroic mirror and after being reflected off a dual dichroic mirror (see Fig. 1). The collimated 100-μm laser beam left the microscope objective and transilluminated the cell under investigation. A first diffraction maximum of the emerging pattern was then projected onto the linear CCD camera through a laser line interference filter (Omega Optical, Inc., Brattleboro, VT) placed in front of the camera to block wavelengths different from the 632.8-nm He–Ne light (i.e., most of the spectrum of the intense flashes). The laser diffraction system measured sarcomere length every 2 ms.

For cell observation and cell length measurments, a CCD video camera (Cohu, Inc., Electronics Div., San Diego, CA) was attached to the side port of the microscope (not shown in Fig. 1). The video signal was recorded and analyzed using a video dimension analyzer, which updated a voltage proportional to cell length every 16.6 ms (Crescent Electronics, Sandy, UT). For comparison of data obtained with either method, cell length measurements were converted to sarcomere length measurements using a resting sarcomere length of 1.85 μm (5). Except for differences in temporal resolution or sensitivity to sarcomere disorganization (see above) the results of cell relengthening or shortening obtained by either method were comparable.

Photolysis: high-power flash unit

To photolyse caged ATP and to induced relengthening in cardiac myocytes, we used a flash unit which discharges electrical energy up to 230 Ws within 1 ms through a short-arc Xenon flashlamp (Chadwick-Helmuth, El Monte, CA). The light was collected by an ellipsoidal mirror (Opti-Forms, Temecula, CA). Light in the desired range of wavelengths (330–410 nm) was reflected off a dichroic mirror (Acton Research Corp., Acton, MA) and focused onto the aperture of a UV-grade liquid light guide positioned in the second focus of the ellipsoidal mirror (Oriel). The liquid light guide represents the standard interface for the input optics in all our experimental setups. This interface provides the modularity and mobility of the flash units as well as other illumination systems. The output aperture of the liquid light guide was then imaged onto the cell using a planoconvex lens and the microscope objective. Wavelength selection was enhanced between the planoconvex lens and the preparation by reflecting the UV light off the dichroic mirror (310–390 nm; CVI Laser Corp., Albuquerque, NM) and the dual-dichroic mirror (310–390 and 610–650 nm; Omega Optical, Inc.) (see Fig. 1).

Photolysis: low-power flash unit

The low-power unit was capable of discharging 7 Ws per flash at rates up to 12 Hz and consisted of commercially available modules mounted in a series of shielding boxes to minimize electromagnetic interference. The short-arc metal-can flashlamp with trigger unit and the high- and low-voltage power supplies were obtained from EG&G, Electro-Optics Div. (Salem, MA). High-voltage capacitors were soldered along a copper bar to give the desired capacitance. The low-power flash unit was used to release ATP gradually to simulate the time course of ATP increase expected during solution changes in experiments with skinned cells.

Cell preparation and solutions

Myocytes were prepared from ventricles of adult guinea pig hearts using an enzymatic procedure as described previously (20). Briefly, guinea pigs (weight ≈350 g) of either sex were injected with 300 U heparin to prevent blood coagulation. Subsequently, the animals were anesthetized by intraperitoneal injection of 25 mg pentobarbital sodium. The hearts were excised quickly and mounted on a Langendorff apparatus for retrograde perfusion with a solution containing 200 μM Ca^{2+} at 35°C. This solution was replaced with nominally calcium-free solution (no added calcium) for 5 min. 25 mg collagenase B (Boehringer-Mannheim Biochemicals, Indianapolis, IN) and 5 mg protease Type XIV (Sigma Chemical Co., St. Louis, MO) were added to 50 ml of the calcium-free solution and perfusion continued in the presence of the enzymes for another 5 min. After perfusion with the enzymes the ventricles were cut into small pieces and gently agitated in the calcium containing solution. Cells were harvested from the supernatant and kept in this solution until they were transferred to the bath solution.

The bath solution had the following composition: 145 mM NaCl, 4 mM KCl, 1 mM $MgCl_2$, 1 mM $CaCl_2$, 10 mM Hepes, 10 mM 2-deoxyglucose, pH 7.4 (adjusted with NaOH). The cells remained in this solution for at least 10 min before the experiments were carried out. To induce complete metabolic blockade, NaCN (2–4 mM) was added from a stock solution of NaCN (600 mM) to a nominally Ca^{2+}-free standard bathing solution (no added calcium, no calcium buffer). The NaCN stock solution was mixed with an equivalent volume of Hepes (1 M) immediately before the experiment to minimize loss of HCN gas. The experiments were performed at room temperature (22–24°C).

The pipette filling solution had the following composition: 120 mM

K-gluconate, 2 mM $MgCl_2$, 10 mM Hepes, 10 mM EGTA, P^3-1-(2-nitrophenyl)ethyladenosine 5'-triphosphate (NPE-caged ATP) (2 mM), reduced glutathione (GSH) (2 mM), pH 7.2 (adjusted with KOH). GSH was added to prevent side-effects of the photolytic byproduct nitrosoacetophenone on actomyosin ATPase (21,22). NPE-caged ATP (disodium salt) was obtained from Molecular Probes, Inc. (Eugene, OR).

Terminology

To avoid confusion we use the following terminology throughout this paper to refer to measured or modeled data. "Relengthening" or "reextension" are used synonymously to describe the increase in cell or sarcomere length. These expressions are distinguished from "relaxation," which refers to the decay of the "rigor force" (see below) inside the cell, a parameter we did not measure in this study but one that underlies the events we investigate. "Shortening force" is the force opposing the internal "restoring force" and would be composed of "active force" due to any cross-bridge cycling plus any "passive rigor force" due to attached rigor bridges that are stretched by the restoring force.

RESULTS

Slow energy deprivation contractions induced by metabolic blockade

After breaking into the cells with the giga-seal pipette, the cytosol was allowed to equilibrate with the pipette filling solution containing the caged ATP compound. The cell was maintained at a fixed holding potential between −50 and −90 mV in the bathing solution containing 10 mM 2-deoxy-glucose. After 10 min, 2 mM NaCN was added to the superfusion solution to induce complete metabolic inhibition and to suppress the synthesis of ATP within the cell. The absence of ATP synthesis with continued cellular consumption lead to a fall of $[ATP]_i$ and a slow energy deprivation shortening of the cell with a velocity of shortening ~10 nm s^{-1} per sarcomere (see Fig. 2, *A* and *B*). A first exposure to NaCN produced the contracture after a delay lasting between 1 and 10 min which appeared to depend on the amount of high-energy substrate within the cell at the time of NaCN exposure. The delay generally seemed to correlate with the yield of the cell isolation procedure (low yield was associated with a short delay indicating low levels of $[ATP]_i$). Without intervention, shortening continued at this slow velocity until a sarcomere length of ~1.4 μm was reached. Further shortening proceeded at a slower velocity (~2.5 nm s^{-1} per sarcomere).

Release of caged ATP with low-power flashes

Fig. 2 *A* shows the reextension of a myocyte from an energy-deprivation contracture when ATP was gradually released by a series of 20 low-power flashes (7 Ws each) within 2 s. The figure shows that before the flash there was a period of steady, slow shortening. At a sarcomere length of 1.6 μm, ATP release was initiated by a burst of flashes. Before relengthening occurred, the cell first shortened at an increased rate during 200 ms. This "recontracture" was followed by a rapid reextension to a sarcomere length of 1.75 μm that was followed

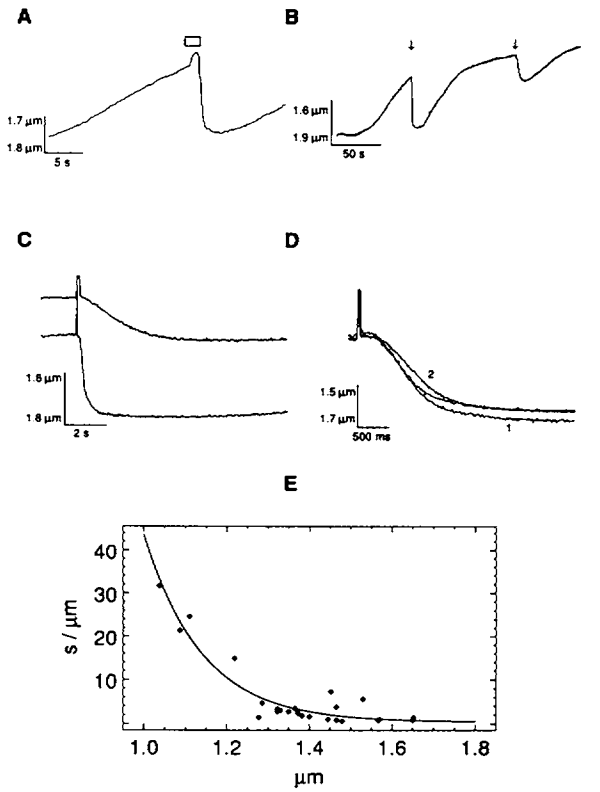

FIGURE 2 Photorelease of ATP induces relengthening of isolated myocytes after energy deprivation contractures. (*A*) Sarcomere length is plotted at a slow time base during an energy-deprivation contracture. During the time indicated by the bar, ATP was released by a series of 20 low-power flashes (7 Ws each). (*B*) The rigor contractures were interrupted by a high-energy flash (↓) (230 Ws) at sarcomere lengths of 1.45 and 1.3 μm, respectively. (*C*) The same reextensions induced by release of ATP (from *B*) are superimposed at a faster time-base. After the flash artefact (at time zero) relengthening was observed in both cases. Relengthening was found to be fast and almost complete when initiated at a sarcomere length of 1.45 μm, but the reextension proceeded slowly and was incomplete when initiated at a sarcomere length of 1.3 μm. (*D*) Three consecutive reextensions produced by different amounts of photo-released ATP are superimposed in one plot. The amount of ATP released for each trace was varied by changing the energy discharged through the flashlamp from 230 Ws (*1*) to 50 Ws (*2*) and again to 230 Ws. (*E*) The dependence of the maximal velocity of relengthening on the sarcomere length before photolysis is illustrated. Inverse velocities are plotted as obtained from pooled experiments (26 reextensions from 15 different cells). Overlapping symbols are invisible. The continuous line is an exponential least-squares fit to the data.

by a second energy-deprivation contracture as the photo-released ATP was consumed. A similar recontracture before relengthening has been described in skinned cells after changing the ATP concentration of the superfusion solution from 0 to 1 mM (14) and is expected to develop before relengthening begins, as outlined below. Rigor shortening at low $[Ca^{2+}]_i$ is believed to develop because rigor bridges, once formed, are able to suppress the tropomyosin inhibition of the acto-myosin interaction and thus facilitate cross-bridge cycling of neighboring cross-bridges (23). As the ATP concentration declines within the cell (due to consumption in the presence of 2-deoxyglucose and NaCN), the rigor state of the cross-bridge cycle becomes more populated. This initially enables cycling of neighboring myosin heads but later, as ATP declines further, leaves fewer cross-bridges able to cycle. In addition to the transient increase in crossbridge cycling with a decreasing [ATP], there is an increase in stiffness that is proportional to the number of rigor cross-bridges formed (see, for example, reference 22). The relation between developed tension and ATP concentration has been observed directly in skinned heart muscle cells and skeletal muscle fibers (22, 24). It gives rise to a bell-shaped dependence of force on ATP concentration with a peak of developed tension near 3 μM MgATP and no force produced at zero MgATP and physiological MgATP, respectively. Consequently, in the present experiments the gradual release of ATP from caged ATP by a series of low-energy flashes was expected to induce a recontracture before relengthening initiated because rigor shortening resumes as the ATP concentration increases from submicromolar levels through the concentration range of maximal force production.

Release of ATP with high-power flashes

Fig. 2 *B* illustrates a high-energy flash experiment at a slow time base with a ventricular myocyte loaded with caged ATP. NaCN was added to the superfusion solution 10 min before the events shown here. Before the flash was activated, sarcomere-length had decreased slowly from 1.85 to 1.45 μm. A single 230-Ws flash induced almost complete relengthening. After 5 s, the cell started to shorten again, presumably because the ATP released by the flash had been consumed by the cell. The next contraction was allowed to proceed to a sarcomere length of 1.3 μm. At 1.4 μm a discontinuity of the shortening velocity was observed, possibly indicating a sudden increase of the internal relengthening force at this sarcomere length. Release of ATP at this shorter sarcomere length induced incomplete relengthening to 1.45 μm. In Fig. 2 *C*, the same two reextensions are superimposed at a higher temporal resolution. Whereas the velocity of relengthening was 0.96 μm · s^{-1} per sarcomere for the first flash, relengthening proceeded significantly slower from a sarcomere length of 1.3 μm (0.07 μm · s^{-1} per sarcomere). In neither case was a recontracture observed, but relengthening started after a delay which outlasted the flash artefact (see also Fig. 2 *D* and Fig. 3 *B*). For reextensions from sarcomere lengths longer than 1.4 μm, the average duration of this delay was 150 ± 25 ms (mean ± SE, n = 13). We do not

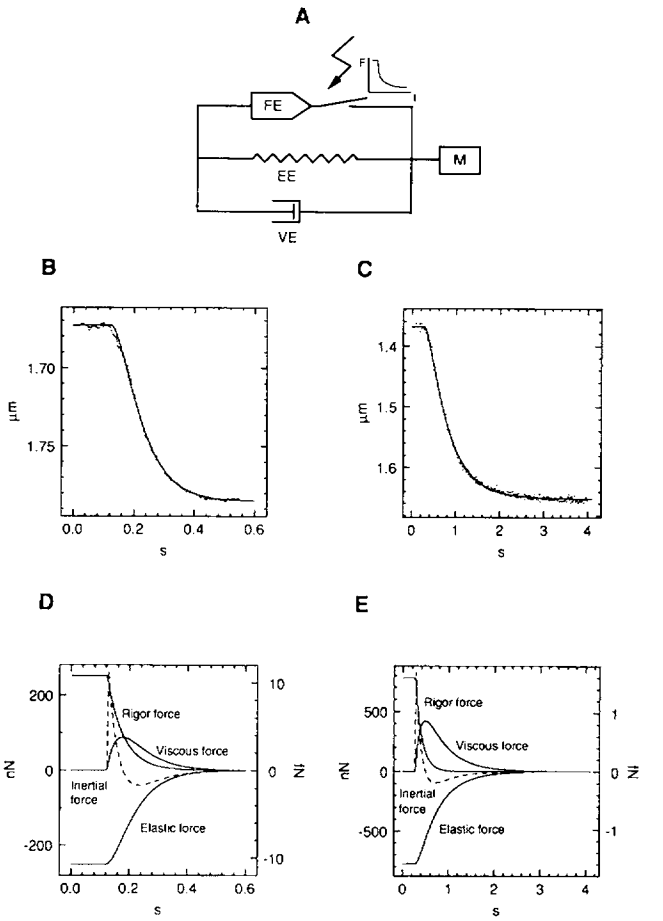

FIGURE 3 The measured data can be described with a simple mechanical model. (*A*) Model. The passively relengthening cell is modeled using the four elements shown. The force-producing element (*FE*) can be disconnected rapidly from the compressed elastic element (*EE*). When the cell length changes, a damping force is generated by a parallel viscous element (*VE*) and the cell mass (*M*) is accelerated. (*B* and *C*) Best fits of the model to measured reextensions from two different sarcomere-lengths. The flash was activated at time zero; the flash artefact has been removed. Note the difference in the time scale for the two plots. (*D* and *E*) The forces corresponding to the reextensions of *B* and *C* were calculated using a published elastic modulus. The time course and the relative magnitude of the rigor force, the viscous force, the elastic force, and the inertial force are shown. The righthand scale applies to the inertial force (*dashed lines*).

know exactly what this delay is due to, but our thinking is as follows: in complete rigor, the number of rigor bridges is greater than the minimum required to balance the relengthening forces within the cell. After a flash (and after dissociation of ADP possibly bound to some cross-bridges) the number of rigor bridges decreases as expected because ATP is able to promote detachment of rigor bridges. But we do not see a change in cell length until the number of rigor bridges has dropped significantly. We imagine that a given rigor bridge is able to be stretched (and thereby generate a counter force) up to a limiting extent. Each rigor bridge is thus able to generate a maximum amount of counterforce before it "breaks" and detaches. Because the displacement of the sarcomere during the stretching of a rigor bridge is so small, we do not detect it with our system. Instead, we observe a delay as the population of rigor bridges is being simultaneously depleted (by high ATP) and being stretched (by a constant amount of relengthening force). This interpretation of the delay would also predict a length dependence of the delay as a result of the increasing number of rigor bridges at shorter sarcomere lengths. (Alternatively, the delay could arise from increased myofilament tangling.) When pairs of records obtained from the same cell but from two different sarcomere lengths were compared, we found a significant increase in the duration with 129 ± 28 ms (mean ± SE, $n = 10$ reextensions) from an average sarcomere length of 1.53 μm, but 309 ± 28 ms when ATP release was initiated at an average sarcomere length of 1.26 μm. As a consequence of this delay, we only observe a single rate constant of relaxation during relengthening, since the more complex changes of rigor force decay occur during the delay of the length signal (22). These considerations have important implications for our mathematical model (see below).

The dependence of the maximal velocity of relengthening on the sarcomere length before photolysis is illustrated in Fig. 2 *E*. Reciprocal maximal velocities (in seconds · microns^{-1}) are plotted versus sarcomere-length. The plot shows pooled data obtained from 26 reextensions in 15 different cells. The continuous line represents an exponential fit to the data points. The average peak velocity of relengthening from sarcomere lengths longer than 1.4 μm, i.e., from cells that did not undergo severe shortening, was 0.77 ± 0.13 μm · s^{-1} per sarcomere (mean ± SE, $n = 13$). It is surprising that the velocity of relengthening from short sarcomere lengths was much slower than from intermediate sarcomere lengths. This indicates that slow relengthening may be a property of highly deformed myocytes which have undergone severe rigor contractions. Extreme rigor contractures seem to proceed beyond the elastic deformability limits of the cell structure. To explain this surprising behavior, we suggest that irreversible "damage" or tangling or subcellular structural elements may result from extreme rigor shortening in unloaded cardiac myocytes. This is consistent with our observation and those of others, that the length does not readily return to control levels after shortening to sarcomere lengths beyond ~1.4 μm. Ultrastructural studies performed on frog skeletal muscle fibers which underwent unloaded contractures have shown that the sarcomeres are indeed extremely shortened and that the myosin filaments appear to be deformed (25).

Is the rigor bridge detachment rate limiting in relengthening?

We can only estimate the amount of released ATP because we have no means at present for making measurements in a single cell under these conditions. For detachment of all rigor cross-bridges, an amount equivalent to the number of myosin heads must (as a minimum) be released by photolysis. We assume the concentration of rigor cross-bridges to be ~200 μM (22). Based on the observation that in some cells we could induce up to five extensions and assuming a supply of unused caged compound from the pipette of 100 μM per minute, we estimate that in our setup one 230-Ws flash photolyses ~20% of the caged compound within the cell, thus giving rise to a concentration jump of ATP up to ~400 μM for the first flash. Apparently, diffusion of unused caged ATP from the pipette into the cell can only partially compensate for the photoconversion of caged ATP and consumption of the released ATP. Therefore, after approximately five flashes (taking place over ~3 min), the supply of caged ATP is exhausted and the cell can no longer be relaxed by the application of UV flashes.

It is important for the analysis of the passive viscoelastic properties of unloaded cardiac myocytes during reextension, that the overall rate of force decay is fast compared with the relengthening process and that detachment is not the rate-limiting step during reextension. To test this hypothesis, we have changed the amount of released ATP by varying the energy discharged through the flashlamp. As outlined in the Discussion, the overall rate of cross-bridge detachment is expected to vary with the concentration of released ATP. If detachment indeed was not the rate-limiting process for relengthening, we would anticipate only minor changes of the relengthening velocity when the ATP concentration jump is reduced. Fig. 2 *D* shows three superimposed reextensions triggered near the same sarcomere length. These records were obtained in a sequence in one cell. The power was changed from 230 (trace 1) to 50 Ws (trace 2) and back again to 230 Ws

(trace without label). The measured maximal relengthening velocities were 0.38, 0.30, and 0.38 $\mu m \cdot s^{-1}$ per sarcomere. The close similarity of the three records despite a nearly fivefold change in released ATP suggests that rigor-bridge detachment is fast compared to the passive relengthening and is not the rate limiting step. This finding also suggests that small (less than fivefold) subcellular nonuniformities of ATP release are insignificant experimentally.

A simple mechanical model can adequately describe the passive behavior of myocytes during relengthening

As outlined above, we were particularly interested in the length dependence of the internal restoring forces in unloaded myocytes. One of our goals was to better define this basic mechanical property of such a widely used preparation. This endeavor may also provide the biophysical basis for the future physiological and pathophysiological investigation of diastolic relaxation events that is a related interest of ours. We thus have also tried to address the question of whether or not the cell length measurements usually performed on this preparation provide an adequate description of the force produced by the unloaded cell. Because only sarcomere lengths and no forces could be measured in our experiments, we developed a mechanical model to describe the recorded data and to estimate the forces involved. Based on ultrastructural studies of the sarcomeres and the dimension of the contractile proteins, we expected to find a sudden change of the elastic modulus of an unloaded cell at a sarcomere length near 1.6 μm (10). At this sarcomere length, the thick myosin filaments begin to touch the Z discs of the sarcomeres. For a first approach, however, we have developed a model based on the assumption of a constant elastic modulus in the range of sarcomere lengths prevailing during twich contractions. We expected that this simple model would not adequately describe our data and that a refined model would have to include a length dependence of the elastic modulus. To our surprise, however, the first very simple model was adequate to describe our data quite well.

We have implemented a mechanical model of the passively relengthening myocyte using the simulation software "Facsimile" (26). Facsimile is designed for the simulation of stiff initial condition problems. In addition, it can also execute parameter fitting runs of a model system to observed data under control of a nonlinear least-squares routine.

A schematic diagram of the model is depicted in Fig. 3*A*. It consists of the following mechanical elements. *FE* is the active element producing the shortening force. An associated "switch" allows a rapid reduction and disconnection of the shortening force from the passive elements (e.g., as would occur after the photorelease of ATP by a light flash). An elastic element (*EE*) is compressed during contractions and generates the intracellular relengthening force that opposes shortening during cross-bridge cycling and that stretches rigor bridges when cycling is negligible. After detachment of a sufficient number of cross-bridges, the elastic element induces relengthening. A viscous element (*VE*) provides a dampening force during reextension. The model also includes a mass (*M*) representing the mass of the cell. Friction between the cell membrane and the coverslip of the bath was not included in the model because we found no difference in the properties of relengthening whether the cells were touching the coverslip or were slightly lifted above the glass surface. Apparently, there is always a thin layer of superfusion solution between the cell and the glass surface, except possibly near the region where the cell is held by the pipette. This model is comparable with an overdamped pendulum returning to its equilibrium position from a mechanical excursion (viscoelastic vibration model).

At any time before and during cellular relengthening, the sum of all forces in this model is always equal to zero. The elastic force $F_{(e)}$, generated by the compressed elastic element, depends on the elastic modulus E of this element (N/m^2), on the cross-sectional area A of the cell (assuming a constant cell volume during contractions) and on cell shortening ($\Delta l/l_0$) negative dimensionless values). The elastic force is calculated using the equation

$$F_{(e)} = EA\frac{\Delta l}{l_0}. \qquad (1)$$

We have modeled the rigor force to decay monoexponentially after a delay. The rationale to choose a monoexponential force decay was based on the assumption, that after the delay between the flash and the onset of relengthening observed in our experiments the more complex changes of rigor force described in skinned skeletal muscle fibers are completed (22). Consequently, only the monoexponential rigor force decay with the relatively low rate will have an influence on relengthening. Thus, the rigor force was calculated to be

$$F_{(r)} = F_{(r_0)}exp\left(\frac{d-t}{\tau}\right), (d-t) = 0 \text{ if } d > t, \qquad (2)$$

where $F_{(r_0)}$ is the rigor force at time = 0, d is the delay, t is time, and τ is the monoexponential time constant of rigor force relaxation. Relengthening of the cell after relaxation was damped by a viscous force proportional to

relengthening velocity

$$F_{(v)} = B\frac{dl}{dl}, \tag{3}$$

where B is the damping constant with units $Ns\ m^{-1}$. The mass of the cell (m) produces an inertial force $F_{(m)}$ proportional to its acceleration according to the equation

$$F_{(m)} = m\frac{d^2l}{dt^2}. \tag{4}$$

The mechanical model and the four forces involved are summarized with the following differential equation

$$F_{(t_0)}exp\left(\frac{d-t}{\tau}\right) + EA\frac{\Delta l}{l_0} + B\frac{dl}{dt} + m\frac{d^2l}{dt^2} = 0. \tag{5}$$

We have used this model to fit the parameters B (damping), d (delay), and τ (rate of decay) to the measured data. The required cell dimensions were measured before the experiment using an eyepiece with a calibrated grating. The mass of the cell was determined based on the cell volume. The value for the elastic modulus near the resting cell length was taken from the literature to be 25 mN/cm^2 (7). Fig. 3 *B* shows a reextension from a small rigor contraction, whereas Fig. 3 *C* represents the best fit of the model to relengthening from an intermediate contraction (note the difference in the time base). The fitted values obtained from the model have subsequently been used to calculate the time course and the relative magnitude of the forces involved. Fig. 3, *D* and *E* show a plot of the resulting simulation runs. Time zero coincides with the flash. Before the flash and during the delay, the rigor force is opposed by the elastic force only, the viscous force and the inertial force are zero. When the cell begins to relengthen after the delay, the inertial force (right-hand ordinate) rises to its peak as the cell mass is accelerated, then returns below zero to result in a relengthening (negative) force. Note, however, that the inertial force is approximately seven orders of magnitude lower than the other forces involved and thus may not contribute much force during reextension. This means, that the elastic relengthening force is essentially balanced by the viscous force and the remaining rigor force. The length-dependent decay of the elastic force to zero reflects the relengthening of the cell back to l_0. As the cell gains relengthening speed, the viscous force increases to its peak and then declines to zero as the cell stops relengthening. This considerable viscous damping would be expected to have a profound influence on the rapid shortening phase in unloaded twitches. Depending on the experimental conditions, peak shortening velocities during twitch contractions are often in the range of the relengthening velocities observed here (1–10 μm · s^{-1} per sarcomere [5, 27]).

Can this model detect discontinuities in the elastic modulus?

As pointed out above, we expected this model to provide only an imperfect description of our measurements. To assess the influence of the putative discontinuity in elastic modulus and to estimate the ability of the model to detect such discontinuities, we simulated reextensions from a sarcomere length of 1.55 to 1.85 μm with a model using two different elastic moduli, a higher one for the range shorter than 1.65 μm and a lower one for sarcomere lengths longer than 1.65 μm. Fig. 4 *A* shows three simulation runs where the ratio of the elastic moduli was varied from 1:1 to 10:1 and 50:1. The elastic moduli used in the simulations were adjusted to result in the same initial restoring force at the sarcomere length maintained before the release (1.55 μm). The parame-

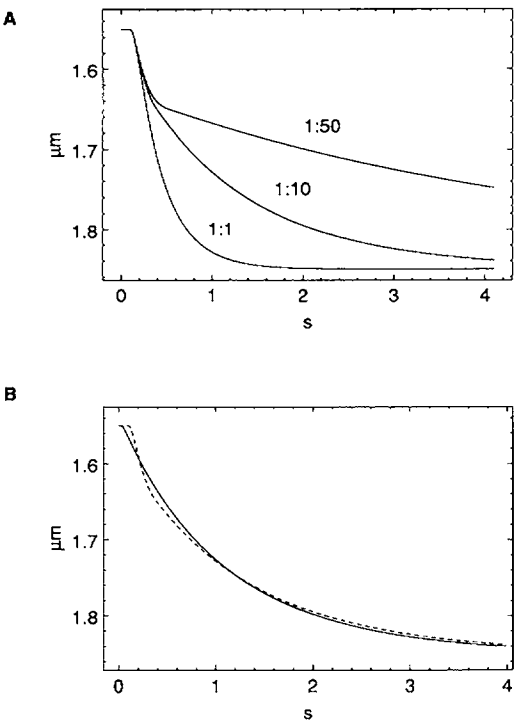

FIGURE 4 Relengthening in the presence of two elastic moduli. (*A*) Model reextensions with a discontinuity in the elastic modulus at 1.65 μm. The three curves represent an equal modulus before and after discontinuity (1:1) and the presence of a 10- and 50-fold increase in the modulus at sarcomere lengths < 1.65 μm. (*B*) The comparison of the best fit obtained with our model (*continuous line*) to the simulated data incorporating two elastic moduli with a ratio of 1:10 (*dashed line*).

ters d (delay) and B (damping) were then fitted to the simulated data. However, attempts to fit the data of simulation runs with an elastic modulus ratio of >10:1 were clearly not satisfactory (see Fig. 4 *B*). This suggests that our data do not support the presence of a significant discontinuity of the elastic modulus between ~1.4 and 1.8 μm during relengthening in unloaded cardiac myocytes. Under these conditions, the force produced by the cell at a steady cell length can be calculated according to Eq. 1. Given the constant volume (V) behavior of the cell

$$V = Al = \text{const.} \tag{6}$$

the cross-sectional area A thus follows the relation

$$A = A_0 \frac{l_0}{(l_0 + \Delta l)}, \tag{7}$$

where l_0 is the resting cell length, A_0 is the cross-sectional area at rest, and Δl represents shortening (negative values). Substitution of A into Eq. 1 gives

$$F_{(e)} = EA_0 \frac{\Delta l}{(l_0 + \Delta l)}. \tag{8}$$

Because E, A_0, and l_0 are constants and Δl assumes negative values for shortening, the relationship between absolute force and cell shortening is described by the following equation

$$F_{(e)} = -K \frac{\Delta s}{(1 - \Delta s)}, \tag{9}$$

where Δs is the relative shortening (positive values) and K is a constant. This equation defines the relationship between cell shortening and developed force and describes a force rising hyperbolically as the cell shortens, as shown in Fig. 5 *A*. Depending on the shortening velocity at a given sarcomere length, the cell also encounters a viscous force. Fig. 5 *B* illustrates the relative magnitude of the elastic force with respect to the viscous force and the dependence of this relation on the shortening velocity for different viscous damping factors. The graph shows the values calculated for a sarcomere length of 1.65 μm (resting sarcomere length 1.85 μm) using elastic moduli and viscous damping factors obtained from the simulation (line *1*; see also Fig. 3 *D*). Two additional curves illustrate the effects of a 10-fold higher (line *2*) and a 10-fold lower (line *3*) damping factor, respectively. Modeled shortening velocities range from 0.01 to 100 μm · s^{-1} per sarcomere. The range of peak shortening velocities usually observed in unloaded twitch contractions (5, 27) is indicated by two vertical dashed lines. At slow shortening velocities, the force

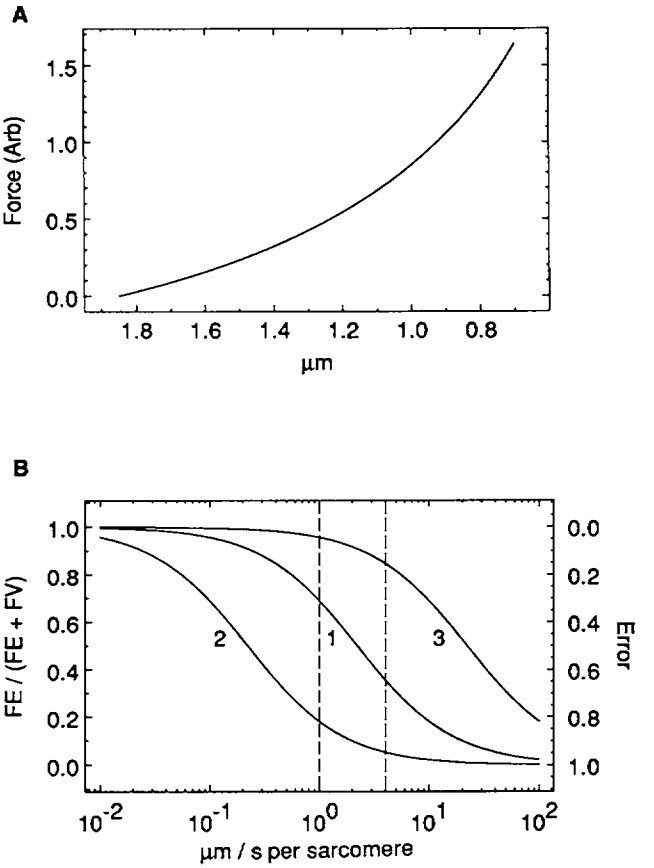

FIGURE 5 Predicted relationship between cell-length, shortening velocity and produced force. (*A*) Assuming a constant volume behavior of the myocyte and the presence of only one elastic modulus the relationship between produced force (in arbitrary units) and steady-state sarcomere length is described by a hyperbolic function. (*B*) The relative magnitude of the elastic force at a sarcomere length of 1.65 μm with respect to the viscous force is plotted for different shortening velocities. Curve *1* shows a simulation using parameters obtained from the mechanical model, curves *2* and *3* illustrate the effects of a 10-fold higher and a 10-fold lower damping factor, respectively. Modeled shortening velocities range from 0.01 μm · s^{-1} to 100 μm · s^{-1} per sarcomere, the dashed vertical lines indicate the range of peak shortening velocities observed in unloaded twitch contractions. The right ordinate represents the error, when the estimate of the force produced by a shortening cell is based on the measured cell length alone.

opposing unloaded cell shortening is almost completely elastic. However, in the range of experimentally observed twitch shortening velocities, only between 70 and 30% of the force is produced to compress elastic elements, whereas the remaining 30 to 70% arise from viscous damping. Thus, estimates of the force from the cell length alone would tend to underestimate the developed force in rapidly shortening cells.

DISCUSSION

Enzymatically isolated ventricular myocytes are a widely used model system to investigate contractile behavior of heart muscle. The mechanical parameter usually measured is either cell or sarcomere length during "unloaded" contractions. Complete relengthening after twitch contractions indicates the presence of an intracellular force restoring the original cell length. Consequently, it is believed that the cell has to develop force during the contraction to overcome this restoring force. The restoring force thus plays an important role in the measured contractile activity. However, it is difficult to measure the internal restoring forces directly over the range prevailing during unloaded twitch contractions in intact cells. The practical approach would be to measure resting stiffness in intact isolated cells (range 1.9–1.5 μm). Unfortunately, with intact cells it is not easily possible to reduce the sarcomere-length below resting values without activating the contractile machinery and thus sacrificing the possibility to measure resting stiffness. Even the technical demanding and elegant measurements of isometric contractile force in single cells cannot provide direct information about the internal restoring forces of unloaded cells (6). Attempts to passively compress skinned cells to achieve sarcomere lengths below ~1.6 μm have resulted in buckling of sarcomeres, have indicated a sharp increase in stiffness at this point (28). In another study with mechanically skinned myocytes the relengthening properties were quite different above and below ~1.6 μm (29). Relengthening, induced by rapidly buffering free Ca^{2+}, occurred in two distinct phases. A rapid reextension to a sarcomere length of 1.6 μm was followed by a very slow relengthening to 1.9 μm. The rapid phase required 600 ms, which is comparable to our observations in intact cells. However, the slow phase lasted ~50 s to complete reextension. This is significantly slower than our observations in intact cells and may be the result of the skinning process as well as consequent changes in the volume and isovolumic behavior of the myofilament lattice. These maneuvers may also lead to the loss or alteration of structures responsible for the restoring force at sarcomere lengths >1.6 μm.

So far the relationship between force production and shortening in unloaded, isolated myocytes is still unknown. The relengthening process itself is induced by intracellular restoring forces. While the relengthening process seems to be a likely source of information on the underlying restoring forces, reextension from twitch contractions exhibits a complicated multiexponential time course (19). This may be the result of multiple processes that remove Ca^{2+} from the cytosol and thereby influence force generation and relaxation.

The recently developed method of releasing biologically active compounds from inactive but light-sensitive precursors ("caged compounds") allows relatively rapid concentration changes of the released compound (τ from microseconds to milliseconds) (30, 31). Making use of the observation that low intracellular ATP concentrations can activate contractions in intact isolated myocytes in the absence of a Ca^{2+} transient (14), we have used photorelease of ATP from caged ATP to investigate the passive relengthening behavior of unloaded cells. The sudden increase in ATP concentration leads to a rapid reduction in the number of rigor bridges inside the cell. This appears to be rapid enough to reduce the rigor stiffness in an almost 'stepwise' manner simplifying the relengthening process into a passive viscoelastic process. This is particularly the case if relengthening begins from intermediate sarcomere lengths (see Fig. 3 *E*), whereas relengthening from very small rigor contractions appears to be rapid enough to be significantly influenced by the decay of the rigor force (see Fig. 3 *D*).

Illumination of caged ATP with UV light induces breakdown of this photolabile compound resulting in the rapid stoichiometric formation of biologically active ATP (rate ~100 s^{-1} [32]). Additional products released are nitrosoacetophenone and one proton (at pH 7). From biochemical rapid kinetic studies with actomyosin (assumed to represent the biochemical equivalent to the cross-bridges in rigor), the following sequence of events is expected to occur after a stepwise increase in [ATP] (for reviews see references 33, 34): ATP is believed to bind to actomyosin with a second order rate constant of ~10^6 $M^{-1} \cdot s^{-1}$. Since the dissociation rate of actomyosin is >1,000 s^{-1}, ATP binding is the rate limiting step at least up to concentration jumps of 1 mM ATP. In fact, the turbidity change associated with the actomyosin dissociation has been used to measure the (slower) rate of ATP release from caged ATP (32). However, under our experimental conditions the biochemical events after photorelease of ATP may be more complicated by the possibility that ADP may rise significantly under conditions of metabolic inhibition. The intracellular concentration of ADP has been estimated in Langendorff-perfused ferret hearts subjected to metabolic blockade. After measuring the ATP and phosphocreatine (PCr) content with nuclear magnetic resonance techniques the ADP concentration was calculated assuming a rapid equilibrium between ADP, ATP, and PCr (35). The ADP concentration appeared to rise transiently up to ~180 μM and became directly detectable. But after prolonged metabolic inhibition, ADP decreased again below the detection limit as ATP reached micromolar

concentrations and energy deprivation contractures developed. In addition, commercially available caged ATP is usually contaminated with ADP. The batch of NPE-caged ATP used in our experiments contained 4.5% ADP, as determined by us with reverse-phase HPLC. Thus, depending on the actual ADP concentration under our experimental conditions, some cross-bridges may have ADP bound. For these cross-bridges the dissociation of ADP rather than the association of ATP may be the rate limiting step for detachment, because ADP would need to dissociate before ATP can bind. This dissociation rate has been determined to limit ATP binding at a rate of $\sim 300\ s^{-1}$ in rat heart actomyosin (36).

However, in the intact cell the decay of the rigor force and not the detachment rate of the cross-bridges is the relevant parameter determining the onset of relengthening. Moreover, reaction rates obtained from solution biochemistry may not directly correlate with those prevailing in intact cells. The three-dimensional organization of the myofilament lattice and the influence of cross-bridge strain on some of the reaction rates have to be taken into account. More direct information about the relaxation of force expected in unloaded myocytes can be inferred from results obtained with laser flash-photolysis of caged ATP in skinned skeletal muscle fibers. In the absence of ADP the decay of rigor tension exhibited a quite complex behavior related to cooperative reattachment of some myosin heads (22). Reattachment resulted in a transient decrease in the rate of relaxation because some reattached cross-bridges were able to generate force. After these complex changes of rigor force were complete (i.e., after ~ 50 ms), the final relaxation exhibited a biexponential time course with a rapid rate of $\sim 110\ s^{-1}$ and a slow rate of $\sim 16\ s^{-1}$. No saturation in detachment rate (determined as the rate of tension convergence after small prestretches or length releases) was found when the amount of ATP released was increased up to ~ 1 mM, indicating that under these conditions ATP binding to actomyosin is the rate limiting step for the overall reaction of rigor-bridge detachment. In the presence of ADP the time course of relaxation was even more complex. A plateau phase of ~ 100 ms duration could be observed before the final relaxation occurred, again with a fast and slow rate (37). The final slow rate of relaxation is similar in the absence and presence of ADP, although the relative extent of the slow component increases as ADP increases (38). From these results we inferred that under our experimental conditions, the overall rate of force relaxation would be faster than the process of passive relengthening. However, the force decay cannot be considered instantaneous and thus has to be included in a model of the relengthening cell (see below).

A mechanical model of reextension from a rigor contraction incorporating a rigor force producing element, an elastic element, a viscous damping element, and the cell mass was adequate to describe the measured data. Simulation runs performed with the parameters obtained from the parameter-fitting routine could subsequently be used to estimate the forces involved, after substituting a resting elastic modulus determined in skinned cells (7). These model calculations show the time course and the interactions of the four forces involved. It becomes apparent that the inertial force to accelerate the cell mass is negligible when compared with the elastic and viscous force. Thus, the relengthening elastic force is essentially balanced by the decaying rigor force and the velocity-dependent viscous damping force. We have extended the model to include a higher elastic modulus at a sarcomere length < 1.65 μm. Such a property was postulated based on the ultrastructure of the sarcomeres and on the findings in skinned cells. At sarcomere lengths below this limit, either the Z-discs have to be deformed or the myosin filaments altered. If shortening below this limit results in an elastic deformation, the effects of the changing elastic modulus is expected to manifest itself during relengthening as well. With the extended mathematical model including two elastic moduli we found, that a sudden change in elastic modulus of > 10-fold would be readily detectable but was not found. We cannot exclude, however, a continuous change of the elastic modulus over the range of sarcomere lengths examined, but such a continuous change in elastic modulus would not affect the usefulness of cell length measurements as an indicator for the developed force. We conclude that the sudden change in elastic modulus in intact cells is either smaller or alternatively that deformations of the myosin molecules or other structural elements occur. This view is supported by the fact that cell shortening during rigor contractions proceeded steadily until a sarcomere length of ~ 1.4 μm was reached (see Fig. 2 *B*). Only at this point was a marked decrease in shortening velocity observed. Considering the force–velocity relationship, this indicates that the cell does not encounter a significant sudden change in load at a sarcomere length of 1.6 μm, but may do so at 1.4 μm. The ultrastructure underlying the decrease of shortening velocity at a sarcomere length of 1.4 μm is unknown to us but may correspond to shortened myosin filaments (39). Thus, thick filament shortening may represent a possible explanation for the absence of a sudden change of elastic modulus at 1.6 μm. The observed decrease in relengthening velocity at very short sarcomere lengths in our experiments indicates that plastic deformation of

subcellular structures occur, at least during severe rigor reaching sarcomere lengths <1.4 μm. Indeed, very slowly reversible A-band compression has been observed when skinned heart cells were first allowed to shorten to an extreme extent for a prolonged time before they were stretched passively with microtools (29). But it is important to note that in severe rigor the cells shortened to lengths never observed during normal unloaded twitches.

In the intact heart, rate and extent of relaxation are important factors determining the compliance during diastole. Recent studies indicate that slowed relaxation and decreased compliance of the heart ("diastolic failure of the heart") might be important factors in early stages of cardiac failure (for review see reference 40). On the other hand, results from intracellular calcium measurements performed in isolated cells indicate that impaired calcium handling of the cells and the SR may be involved in the increased stiffness during early diastole under different pathological conditions (41, 42). In addition to its importance for the interpretation of unloaded contractions in isolated myocytes, knowledge about the viscoelastic properties of isolated cells might thus be a significant prerequisite for our understanding of the possible effects of processes controlling subcellular calcium dynamics during relaxation.

In conclusion, the results of our experiments and our modeling indicate that sarcomere or cell length are reasonable parameters to measure to estimate the force produced by a single heart muscle cell in the steady state. This force is approximately proportional to the extent of cell shortening and proportional to the cross-sectional area of the cell. Given a constant cell volume during contractions, the force thus rises in a hyperbolic fashion as the cell shortens. Additionally, however, viscous forces may contribute significantly to the overall force during rapid length changes and therefore lead to an important underestimation of the force produced during rapid contractions.

We would like to thank W. G. Sinclair and W. Knapik for their support and assistance in designing and building the optical mounting hardware.

The work was supported by a fellowship from the Swiss National Science Foundation (87-30 BE) to E. Niggli and National Institutes of Health grants (HL36974 and HL25675) to W. J. Lederer.

Received for publication 4 May 1990 and in final form 2 January 1991.

REFERENCES

1. Hamill, O. P., A. Marty, E. Neher, and A. Sakmann. 1984. Improved patch-clamp techniques for high resolution current recording from cells and cell-free membrane patches. *Pfluegers Arch. Eur. J. Physiol.* 391:85–100.
2. Cannell, M. B., J. R. Berlin, and W. J. Lederer. 1987. Effect of membrane potential changes on the calcium transient in single rat cardiac muscle cells. *Science (Wash. DC).* 238:1419–1423.
3. Wier, W. G., M. B. Cannell, J. R. Berlin, E. Marban, and W. J. Lederer. 1987. Cellular and subcellular heterogeneity of $[Ca^{2+}]_i$ in single heart cells revealed by fura-2. *Science (Wash. DC).* 235:325–328.
4. Boyett, M. R., M. Moore, B. R. Jewell, R. A. P. Montgomery, M. S. Kirby, and C. H. Orchard. 1988. An improved apparatus for the optical recording of contraction of single heart cells. *Pfluegers Arch. Eur. J. Physiol.* 413:197–205.
5. Niggli, E. 1987. Mechanical parameters determined in dispersed ventricular heart cells. *Experientia (Basel).* 43:1150–1153.
6. Tung, L., and M. Morad. 1986. Contractile force of single heart cells compared with muscle strips of frog ventricle. *Am. J. Physiol.* 255:H111–H120.
7. Roos, K. P., and A. J. Brady. 1989. Stiffness and shortening changes in myofilament-extracted rat cardiac myocytes. *Am. J. Physiol.* 256:H539–H551.
8. Julian, F. J., and M. R. Sollins. 1975. Sarcomere length-tension relations in living rat papillary muscle. *Circ. Res.* 37:299–308.
9. ter Keurs, H. E. D. J., W. H. Rijnsburger, R. van Heuningen, and M. J. Nagelsmit. 1980. Tension development and sarcomere length in rat cardiac trabeculae. *Circ. Res.* 46:703–714.
10. Severs, N. J., A. M. Slade, T. Powell, V. W. Twist, and G. E. Jones. 1985. Morphometric analysis of the isolated calcium-tolerant cardiac myocyte: organelle volumes, sarcomere length, plasma membrane surface folds, and intramembrane particle density and distribution. *Cell Tissue Res.* 240:159–168.
11. Fabiato, A., and F. Fabiato. 1975. Dependence of the contractile activation of skinned cardiac cells on the sarcomere length. *Nature (Lond.).* 256:54–56.
12. Bridge, J. H. B., K. W. Spitzer, and P. R. Ershler. 1988. Relaxation of isolated ventricular cardiomyocytes by a voltage-dependent process. *Science (Wash. DC).* 241:823–825.
13. Bers, D. M., and J. H. B. Bridge. 1989. Relaxation of rabbit ventricular muscle by Na-Ca exchange and sarcoplasmic reticulum Ca-pump: ryanodine and voltage sensitivity. *Cir. Res.* 65:334–342.
14. Nichols, C. G., and W. J. Lederer. 1990. The role of ATP in energy-deprivation contracture in unloaded rat ventricular myocytes. *Can. J. Physiol. Pharmacol.* 68:183–194.
15. Niggli, E., and W. J. Lederer. 1990. Relengthening from rigor observed in isolated cardiac myocytes after photorelease of ATP. *Biophys. J.* 57:552*a*. (Abstr.)
16. Cannell, M. B., and W. J. Lederer. 1986. A novel experimental chamber for single-cell voltage clamp and patch-clamp application with low electrical noise and excellent temperature and flow control. *Pfluegers Arch. Eur. J. Physiol.* 406:536–539.
17. Niggli, E., and W. J. Lederer. 1990. Real-time confocal microscopy and calcium measurements in heart muscle cells: towards the development of a fluorescence microscope with high temporal and spatial resolution. *Cell Calcium.* 11:121–130.
18. Roos, K. P., A. C. Bliton, M. J. Patton, and S. T. Taylor. 1989. Regional differences during unloaded contractions of isolated rat cardiac myocytes. *Biophys. J.* 55:268*a*. (Abstr.)
19. Niggli, E. 1988. A laser diffraction system for long-term sarcomere length measurements in isolated myocytes. *Pfluegers Arch. Eur. J. Physiol.* 411:462–468.

20. Mitra R., and M. Morad. 1985. A uniform enzymatic method for dissociation of myocytes from hearts and stomachs of vertebrates. *Am. J. Physiol.* 249:H1056–1060.

21. Kaplan, J. H., B. Forbush, and J. F. Hoffman. 1978. Rapid photolytic release of adenosine 5′-triphosphate from a protected analogue: utilization by the Na:K pump of human red blood cell ghosts. *Biochemistry.* 17:1929–1935.

22. Goldman, Y. E., M. G. Hibberd, and D. R. Trentham. 1984. Relaxation of rabbit psoas muscle fibres from rigor by photochemical generation of adenosine-5-triphosphate. *J. Physiol. (Lond.).* 354:577–604.

23. Bremel, R. D., and A. Weber. 1972. Cooperation within actin filament in vertebrate skeletal muscle. *Nat. New Biol.* 238:97–101.

24. Fabiato, A., and F. Fabiato. 1975. Effects of magnesium on contractile activation of skinned cardiac cells. *J. Physiol. (Lond.).* 249:497–517.

25. Huxley, H. 1990. An explanation of the A-band shortening artifact in vertebrate striated muscle. *Biophys. J.* 57:543*a*. (Abstr.)

26. Chance, E. M., A. R. Curtis, I. P. Jones, and C. R. Kirby. 1977. Facsimile: A Computer Program for Flow and Chemistry Simulation, and General Initial Value Problems. UK Atomic Energy Authority, Harwell, UK.

27. Krueger, J. W., D. Forletti, and B. A. Wittenberg. 1980. Uniform sarcomere shortening behavior in isolated cardiac muscle cells. *J. Gen. Physiol.* 76:587–607.

28. Iwazumi, T. 1987. A new method to attach single cardiac myocyte to transducers. *Biophys. J.* 51:479*a*. (Abstr.)

29. Fabiato, A., and F. Fabiato. 1976. Dependence of calcium release, tension generation and restoring forces on sarcomere length in skinned cardiac cells. *Eur. J. Cardiol.* 4(Suppl.):13–27.

30. Gurney, A. M., and H. A. Lester. 1987. Light-flash physiology with synthetic photosensitive compounds. *Physiol. Rev.* 67:583–617.

31. McCray, J. A., and D. R. Trentham. 1989. Properties and uses of photoreactive caged compounds. *Annu. Rev. Biophys. Chem.* 18:239–270.

32. McCray, J. A., L. Herbette, T. Kihara, and D. R. Trentham. 1980. A new approach to time-resolved studies of ATP-requiring biological systems: laser flash photolysis of caged ATP. *Proc. Natl. Acad. Sci. USA.* 77:7237–7241.

33. Homsher, E., and N. C. Millar. 1990. Caged compounds and striated muscle contraction. *Annu. Rev. Physiol.* 52:875–896.

34. Hibberd, M. G., and D. R. Trentham. 1986. Relationships between chemical and mechanical events during muscular contraction. *Annu. Rev. Biophys. Biophys. Chem.* 15:119–161.

35. Allen, D. G., P. G. Morris, C. H. Orchard, and J. S. Pirolo. 1985. A nuclear magnetic resonance study of metabolism in the ferret heart during hypoxia and inhibition of glycolysis. *J. Physiol. (Lond.).* 361:185–204.

36. Siemanowski, R. F., M. O. Wiseman, and H. D. White. 1985. ADP dissociation from actomyosin subfragment 1 is sufficiently slow to limit the unloaded shortening velocity in vertebrate muscle. *Proc. Natl. Acad. Sci. USA.* 82:658–662.

37. Dantzig, J. A., M. G. Hibberd, Y. E. Goldman, and D. R. Trentham. 1984. ADP slows cross-bridge detachment rate induced by photolysis of caged ATP in rabbit psoas muscle fibers. *Biophys. J.* 45:8*a*. (Abstr.)

38. Woodward, S. K. A., and M. A. Ferenczi. 1990. The rate of ADP release from muscle cross-bridges. *Biophys. J.* 57:540*a*. (Abstr.)

39. Periasamy, A., D. H. Burns, D. N. Holdren, G. H. Pollack, and K. Trombitás. 1990. A-band shortening in single fibers of frog skeletal muscle. *Biophys. J.* 57:815–828.

40. Gilbert, J. C., and S. A. Glantz. 1989. Determinants of left ventricular filling and of the diastolic pressure-volume relation. *Circ. Res.* 64:827–852.

41. Lakatta, E. G. 1987. Cardiac muscle changes in senescence. *Annu. Rev. Physiol.* 49:519–531.

42. Gwathmey, J. K., L. Copelas, R. MacKinnon, F. J. Schoen, M. D. Feldman, W. Grossmann, and J. P. Morgan. 1987. Abnormal intracellular calcium handling in myocardium from patients with end-stage heart failure. *Circ. Res.* 61:70–76.